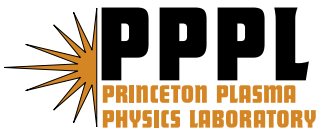

Princeton Plasma Physics Laboratory

PPPL-

PPPL-



Prepared for the U.S. Department of Energy under Contract DE-AC02-09CH11466.

Princeton Plasma Physics Laboratory

Report Disclaimers

Full Legal Disclaimer

This report was prepared as an account of work sponsored by an agency of the United States Government. Neither the United States Government nor any agency thereof, nor any of their employees, nor any of their contractors, subcontractors or their employees, makes any warranty, express or implied, or assumes any legal liability or responsibility for the accuracy, completeness, or any third party's use or the results of such use of any information, apparatus, product, or process disclosed, or represents that its use would not infringe privately owned rights. Reference herein to any specific commercial product, process, or service by trade name, trademark, manufacturer, or otherwise, does not necessarily constitute or imply its endorsement, recommendation, or favoring by the United States Government or any agency thereof or its contractors or subcontractors. The views and opinions of authors expressed herein do not necessarily state or reflect those of the United States Government or any agency thereof.

Trademark Disclaimer

Reference herein to any specific commercial product, process, or service by trade name, trademark, manufacturer, or otherwise, does not necessarily constitute or imply its endorsement, recommendation, or favoring by the United States Government or any agency thereof or its contractors or subcontractors.

PPPL Report Availability

Princeton Plasma Physics Laboratory:

<http://www.pppl.gov/techreports.cfm>

Office of Scientific and Technical Information (OSTI):

<http://www.osti.gov/bridge>

Related Links:

[U.S. Department of Energy](#)

[Office of Scientific and Technical Information](#)

[Fusion Links](#)

Feasibility Studies of Alpha-Channeling in Mirror Machines

A. I. Zhmoginov* and N. J. Fisch†

Princeton Plasma Physics Laboratory, Princeton University, Princeton, NJ 08543, USA

The linear magnetic trap is an attractive concept both for fusion reactors and for other plasma applications due to its relative engineering simplicity and high-beta operation. Applying the α -channeling technique to linear traps, such as mirror machines, can benefit this concept by efficiently redirecting α particle energy to fuel ion heating or by otherwise sustaining plasma confinement, thus increasing the effective fusion reactivity. To identify waves suitable for α -channeling a rough optimization of the energy extraction rate with respect to the wave parameters is performed. After the optimal regime is identified, a systematic search for modes with similar parameters in mirror plasmas is performed, assuming quasi-longitudinal or quasi-transverse wave propagation. Several modes suitable for α particle energy extraction are identified for both reactor designs and for proof-of-principle experiments.

I. INTRODUCTION

Alpha particles born through D-T fusion reactions carry 20% of the overall fusion energy. The energy of the α particle population trapped in a mirror fusion reactor largely dissipates through collisions with electrons or it may excite plasma instabilities (see, for example, [1–7]). The collisional relaxation of α particles occurs on a characteristic α -electron collisional time of order of a second and results in fusion ash buildup. Plasma instabilities excited by α particles, in turn, heat the background plasma [8–10] and increase the plasma transport, which also increases the wall heat load.

Alpha-channeling is a wave-particle manipulation technique, which might be capable of inducing α particle flows in phase space leading to quick α ejection accompanied by α particle cooling. As a result, the energy with which α particles are born can be transferred to the waves and then used to sustain the fusion reaction in the device. The channeling of the α power in one simple mirror configuration [11] at ignition has been estimated [12] to increase, potentially, the effective fusion reactivity by a factor of 2.8.

In this paper, we discuss and reformulate the results of our previous studies concerning α -channeling in mirror machines. In addition, using a more convenient set of variables compared to those used in Ref. 13, we rederive the ray-tracing equations for quasi-longitudinal and quasi-transverse waves suitable for α -channeling. Numerical simulations of α -channeling in a mirror machine

outlined in Ref. 14 supported the feasibility of using α -channeling concept proposed in Refs. 12 and 15 in practical open-ended devices. A rough optimization of α -channeling efficiency with respect to rf region parameters (not constrained by the plasma dispersion relation) was also presented in Ref. 14. In a subsequent study [13], the search for the weakly-damped localized modes in plasmas was addressed and two distinct waves suitable for α -channeling were identified in two practical mirror devices [16, 17]. The method of the wave search used in Ref. 13 is rederived here using a more convenient set of coordinates matching the topology of the magnetic field lines and lines orthogonal to them.

The paper is organized as follows. In Sec. II, we discuss the α -channeling concept and its application to open-ended devices. In Sec. III, previous results concerning the optimization of the α -channeling efficiency with respect to rf region parameters are discussed. In Sec. IV, we discuss how the search for the waves suitable for α -channeling can be conducted. We rederive the ray-tracing equations for the quasi-longitudinal and the quasi-transverse waves using canonical curvilinear coordinates and then use these results to formulate a method suitable for identifying spatially localized weakly-damped modes. In Sec. V, we discuss the modes suitable for α -channeling identified in two practical open-ended designs [16, 17] and in the LAPD device [18]. Section VI summarizes our conclusions.

*Electronic address: azhmogin@princeton.edu

†Electronic address: fisch@princeton.edu

II. ALPHA-CHANNELING IN MIRROR MACHINES

The α -channeling effect occurs when α particles born through fusion reactions diffuse along one-dimensional paths in the phase space (\vec{r}, \vec{p}) due to resonant interaction with electromagnetic waves. If the diffusion induced along the path is suppressed at high energy, whereas at low-energy there is an effective particle “sink”, the interaction with the waves will result in the ejection of the cold α particles from the system and the simultaneous transfer of their initial energy to the waves, thereby accomplishing the so-called “ α -channeling” effect [19]. The quick α particle ejection leads to fusion ash removal, while by coupling the amplified wave to the background plasma species, it is possible to redirect extracted energy to the plasma, thus suppressing the instabilities and increasing the effective fusion reactivity compared to the typical scenario, in which α particles heat plasma by slowing down collisionally on electrons [12].

The α -channeling effect might be achieved in a mirror machine by arranging several rf regions along the device length. If the wave frequency ω is approximately equal to the n^{th} harmonic of the α particle cyclotron frequency Ω , the wave will be resonantly coupled to the α particles having a parallel velocity $v_{\parallel} = \vec{v} \cdot \vec{B} / |\vec{B}| = v_{\parallel \text{res}}$ given by:

$$v_{\parallel \text{res}} = \frac{\omega - n\Omega}{k_{\parallel}}, \quad (1)$$

where \vec{v} is an α particle velocity and \vec{B} is the magnetic field.

If the wave amplitude is large enough, the resonant α particle dynamics becomes stochastic. Assuming a slab geometry approximation, one can show using the canonical perturbation theory [20] that the corresponding particle random walk is constrained to a one-dimensional curve in the unperturbed action variable space [21]:

$$\Delta v_{\parallel} \approx \frac{k_{\parallel} \Delta \mu}{nm}, \quad (2)$$

$$\Delta X \approx \frac{k_{\perp} \Delta \mu}{nm\Omega}, \quad (3)$$

where it is assumed that the perpendicular (to the magnetic field) component \vec{k}_{\perp} of the wave vector \vec{k} is directed along \vec{y}_0 , X and Y are the particle gyrocenter coordinates, \vec{B} is directed along z , $k_{\parallel} = \vec{k} \cdot \vec{B} / |\vec{B}|$ and μ is the magnetic moment of the particle. Note that the particle excursion given by Eq. (2) is directed along the resonance surface $\omega - n\Omega - k_{\parallel} v_{\parallel} = 0$ only if $k_{\parallel} = 0$. In

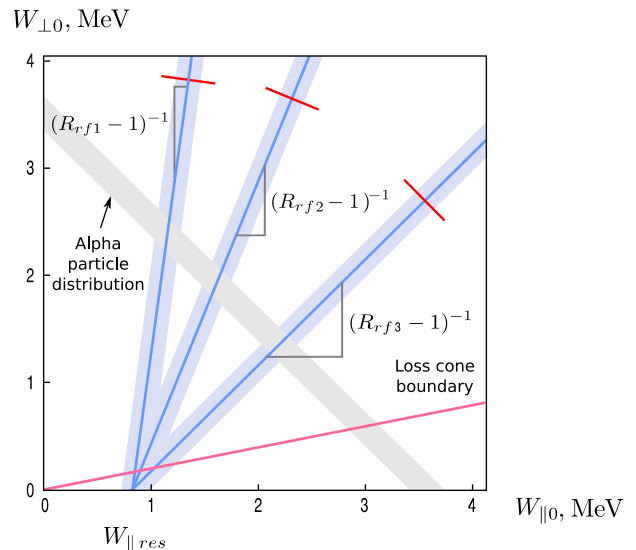


FIG. 1: (Color online) Arrangement of the diffusion paths (bars intersecting at $W_{\parallel} \approx W_{\parallel \text{res}}$) in the midplane energy space. Born through the fusion reaction α particles diffuse along the paths limited at high energies (limitation is schematically shown with the short segments) and leave the device through the loss cone at the intersection points with the paths [with the energy $W \sim W_{\parallel \text{res}} = (m/2)(\omega - n\Omega)^2 / k_{\parallel}^2$].

other words, if $k_{\parallel} = 0$, the resonance condition is satisfied even if the change of the particle energy is substantial. For simplicity in choosing diffusion paths, namely in order to be sure that the particles in resonance remain in resonance, we proceed in the following assuming that $k_{\parallel} \ll k_{\perp}$. However, this condition is not strictly necessary for α -channeling, particularly when there are multiple rf regions in inhomogeneous fields.

Thus, the particle parallel velocity change will be small compared to the characteristic perpendicular velocity change if $k_{\parallel} \ll k_{\perp}$. Since the wave-particle interaction occurs in the region where the resonance condition is satisfied, but not necessarily in the midplane, the diffusion path equation in the midplane energy space turns out to be given by [14]:

$$W_{\parallel}^0 \approx \frac{m}{2} \left(\frac{\omega - n\Omega}{k_{\parallel}} \right)^2 + W_{\perp}^0 (R_{\text{rf}} - 1), \quad (4)$$

where W_{\parallel}^0 and W_{\perp}^0 are the particle’s parallel and perpendicular energies at the midplane correspondingly, and R_{rf} is the mirror ratio at the rf region location. If the α particle resonant velocity is nonzero, such a diffusion path intersects the loss cone (see Fig. 1). Since the particle heating along the path can be limited for $k_{\perp} \rho \gtrsim 1$ [14], where ρ is the α particle gyroradius, particle cooling ac-

accompanied by the particle ejection into the loss cone can be observed in this system. In order to affect a wide range of α particle pitch angles, it is further proposed to use several diffusion paths with different slopes as shown in Fig. 1. More general configurations of diffusion paths, including intersecting networks of paths, were considered [22], however, the highest α -channeling efficiency was demonstrated for the system of paths depicted on Fig. 1. In the following section, a rough numerical optimization of the α -channeling efficiency with respect to the rf region parameters is outlined.

III. OPTIMIZATION WITH RESPECT TO RF REGION PARAMETERS

The conceptual picture of α -channeling discussed in the previous section can be affected by such non-ideal effects as an inhomogeneous background magnetic field, a finite wave spectrum, a finite diffusion path width (essential to affect a large portion of the α particle population), nonlinear effects, and particle phase correlations. The influence of these effects on the feasibility of α -channeling in practical mirror machines can be studied by performing a rough numerical optimization of the α -channeling efficiency with respect to the rf region parameters. As a first step, the numerical optimization discussed in Ref. 14 was performed without accounting for wave dispersion in mirror machine plasmas. The next step, of course, is to search for plasma waves with parameters close to optimal, as discussed in Sec. IV.

The most straightforward approach to the simulation of the α particle dynamics interacting with a wave in a mirror machine is a solution of the Newtonian equations of the α particle motion:

$$m\dot{\vec{v}} = \frac{q}{c}\vec{v} \times \vec{B} + q\vec{E}, \quad (5)$$

where m is the α particle mass, q is the charge, c is the speed of light, and \vec{B} , \vec{E} are the fixed magnetic and electric fields correspondingly. Being the most accurate model of the particle motion considered in Ref. 14, Eq. (5) requires the largest computational time. An approach requiring less computational resources, based on an approximate model, is to calculate the resonant interaction of α particles with an electrostatic wave (see Eqs. (2–5) of Ref. 14).

Simulations of a large number of particles can be performed by simulating a particle random-walk in reduced phase space, a state in which is described by the particle

magnetic moment μ , the parallel momentum p_{\parallel} , the radial position r and the time t when the particle passes the midplane. The change of the particle state $\vec{s} = (\mu, p_{\parallel}, r, t)$ on a single axial bounce is given in this model by expression:

$$\vec{s}_{n+1} = \vec{s}_n + \vec{f}(\vec{s}_n) + \vec{d}(\vec{s}_n)\vec{w}, \quad (6)$$

where \vec{f} and \vec{d} define, respectively, the averaged and stochastic components of the kick that the particle receives from the wave in a single axial bounce time, \vec{w} is a 4-dimensional vector such that $\langle w_i \rangle = 0$, $\langle w_i w_j \rangle = \delta_{ij}$, and \vec{s}_i is the particle state on the n^{th} midplane crossing. To further simplify the model, one can neglect the random terms in the time excursion and assume that the particle radial excursion Δr is related to the change of the particle magnetic moment $\Delta\mu$ by [23]:

$$\Delta r \approx \frac{\ell \Delta\mu}{nrm\Omega}, \quad (7)$$

where ℓ is the wave azimuthal wave number. The remaining components of \vec{f} and \vec{d} can be either found by employing the bounce-averaged quasilinear diffusion theory [24], or calculated numerically for each rf region using Eq. (5) or Eqs. (2–5) of Ref. 14.

Numerical simulations of α particle motion in a mirror machine in the presence of several electrostatic waves were presented in Ref. 14, where it was shown that up to 60% of the total α particle energy can, in principle, be extracted from a practical open-ended fusion device. Specifically, simulations show that 60% of the initial α particle energy can be redirected to the wave in 300 ms. The remaining 40% of the energy is accounted in two ways: (a) some of this energy leaves the device with the unconfined α particles and (b) the deeply trapped α particles simply stay in the device and give up their energy to the other plasma species. A rough optimization of α -channeling efficiency with respect to rf region parameters (ignoring restrictions imposed by the plasma dispersion relation) was performed and the optimal wave parameters were identified. The fuel ion ejection by the rf regions was shown to be weak, while the ion injection mechanism employing the energy of the same waves which were used for α -channeling [12] was demonstrated [14]. It should be emphasized that these simulations were done for ideal waves, just to answer the question of whether any waves, not necessarily realistic waves, could produce a significant α -channeling effect. With the answer to this question positive, it is then important to find suitable waves. We outline such a search in the next section.

IV. SEARCH FOR WAVES

The numerical optimizations of the α -channeling efficiency discussed in Sec. III were performed under the assumption that $k_{\parallel} \ll k_{\perp}$ and $\omega \approx \Omega$. The simulations confirmed that in order to maximize the extracted energy, the wave performing α -channeling should interact with the deeply-trapped α particles and k_{\perp} must satisfy $k_{\perp} \rho \gtrsim 1$. Furthermore, the wave amplitude should be sufficiently large to expel α particles out of the device over a time much smaller than the typical α -electron collisional relaxation time.

If the wave damping is strong, significant energy is required to excite the waves, possibly even larger than the energy extracted from α particles using this wave. Therefore, the fusion reaction rate affects the maximum allowed wave damping rate. Ideally, the wave damping rate should be approximately equal to the wave growth rate due to the α particle energy extraction. In the following, we assume that the wave growth rate is small, so that the excitation of a localized weakly-damped mode trapped in the device core is necessary. This confines our search significantly.

Weakly-damped modes satisfying these conditions can be found assuming the validity of the geometrical optics approximation and restricting the search to the waves propagating primarily along (quasi-longitudinal waves) or transverse (quasi-transverse waves) to the magnetic field lines. We also assume that the device is axisymmetric and fix the azimuthal wave number ℓ . A method of identifying such modes is described in Ref. 13, where several potential mode candidates existing in practical mirror designs are identified. Here, using a more systematic approach than that used in Ref. 13, we rederive the ray-tracing equations for the quasi-longitudinal and the quasi-transverse waves, making more clear the mode search algorithm.

The ray-tracing equations for quasi-longitudinal and quasi-transverse waves can be derived by considering first the ray-tracing equations in (r, z, k_r, k_z) coordinates:

$$\dot{r} = \frac{\partial \mathcal{D}}{\partial k_r}, \quad \dot{k}_r = -\frac{\partial \mathcal{D}}{\partial r}, \quad (8)$$

$$\dot{z} = \frac{\partial \mathcal{D}}{\partial k_z}, \quad \dot{k}_z = -\frac{\partial \mathcal{D}}{\partial z}, \quad (9)$$

where $\mathcal{D}(k_r, k_z, r, z; \omega)$ is a local dispersion relation obtained from the original $\mathcal{D}(k_x, k_y, k_z, x, y, z; \omega)$ by substituting $x = r \cos \phi$, $y = r \sin \phi$, $k_x = k_r \cos \phi - \ell r^{-1} \sin \phi$, and $k_y = k_r \sin \phi + \ell r^{-1} \cos \phi$. The motions of the wave

packet along and across the magnetic field lines can be decoupled by introducing new coordinates (R, η) such that R and η are constant along the magnetic field lines and along the curves orthogonal to them correspondingly. Requiring that $R(r, z=0) = r$, $\eta(r=0, z) = z$, $\partial R/\partial r = -\alpha b_z$, $\partial R/\partial z = \alpha b_r$, $\partial \eta/\partial r = \beta b_r$, and $\partial \eta/\partial z = \beta b_z$, where $\vec{b} = (b_r, b_z)$ is a unit vector field directed along the magnetic field lines, one can calculate functions α and β . In particular, considering a divergence-free magnetic field given by $B_r = -r\mathcal{B}(z)'/2$ and $B_z(r, z) = \mathcal{B}(z)$, where $\mathcal{B}(z)$ is a function defining magnetic field profile along the device axis, one obtains:

$$\alpha = \sqrt{\frac{\mathcal{B}(z)}{\mathcal{B}(0)}} \left(1 + \frac{r^2 \mathcal{B}'^2}{8\mathcal{B}^2} \right) + O\left(\frac{r^4}{L^4}\right), \quad (10)$$

$$\beta = 1 - r^2 \frac{\mathcal{B}''(z)}{\mathcal{B}(z)} + \frac{3r^2 \mathcal{B}'^2(z)}{8\mathcal{B}^2(z)} + O\left(\frac{r^4}{L^4}\right), \quad (11)$$

where we assumed that the characteristic device radius is much smaller than the device length L . The important property of this coordinate transformation is that the basis vectors \vec{e}_R and \vec{e}_η are orthogonal when the original basis (\vec{e}_r, \vec{e}_z) is orthonormal [40]. The metric tensor \bar{g}_{ij} in the new coordinates is diagonal and $\bar{g}_{RR} = \vec{e}_R \cdot \vec{e}_R = \alpha^{-2}$, $\bar{g}_{\eta\eta} = \vec{e}_\eta \cdot \vec{e}_\eta = \beta^{-2}$. Note that even though the lines of constant R coincide with the lines of constant magnetic flux, the new coordinates (R, η) are different from the flux coordinates (ψ, ζ) [25]. In particular, the magnetic flux ψ is a non-linear function of R and the linear coordinate along the magnetic field line ζ is equal to η only in the lowest order in r/L .

Making a canonical transformation in \mathcal{D} from (r, z) to (R, η) using a generating function

$$\Phi(r, z, k_R, k_\eta) = k_R R(r, z) + k_\eta \eta(r, z), \quad (12)$$

one obtains that $k_r = k_R \partial R/\partial r + k_\eta \partial \eta/\partial r$ and $k_z = k_R \partial R/\partial z + k_\eta \partial \eta/\partial z$. Substituting the expressions for $R(r, z)$ and $\eta(r, z)$ here, one finally obtains for k_R and k_η [41]:

$$k_R = \frac{\hat{b}_r k_z - \hat{b}_z k_r}{\alpha} = \frac{k_n}{\alpha}, \quad (13)$$

$$k_\eta = \frac{\hat{b}_r k_r + \hat{b}_z k_z}{\beta} = \frac{k_{\parallel}}{\beta}, \quad (14)$$

where $k_{\parallel} = \vec{b} \cdot \vec{k}$ and $k_n^2 = |\vec{k}|^2 - k_{\parallel}^2$.

The new coordinates (R, η) and the new momenta (k_R, k_η) form a canonical set of coordinates and therefore:

$$\dot{k}_R = -\partial \mathcal{D}/\partial R, \quad \dot{R} = \partial \mathcal{D}/\partial k_R, \quad (15)$$

$$\dot{k}_\eta = -\partial \mathcal{D}/\partial \eta, \quad \dot{\eta} = \partial \mathcal{D}/\partial k_\eta. \quad (16)$$

The dispersion relation $\mathcal{D}(k_n, k_{\parallel}, r, z)$ can be transformed to the new variables by replacing k_{\parallel} with βk_{η} , k_n with αk_R , and by substituting the known expressions for $r(R, \eta)$ and $z(R, \eta)$. Note that the system (15), (16) is identical to the more complicated system of equations (3-6) of Ref. 13. Here, however, the curvatures of the magnetic field lines and the lines orthogonal to them enter the wave packet motion equations transparently through α and β , and the derivation of the approximate equations can be carried out by replacing these dependencies with the lowest-order terms from Eqs. (10) and (11).

In the general case, the dynamics governed by the two-dimensional Hamiltonian $\mathcal{D}(k_R, k_{\eta}, R, \eta)$ can be very complex. However, there are two special cases, in which it can be simplified significantly. In these cases, the dynamics in k_R and R variables is much slower (quasi-longitudinal wave) or much faster (quasi-transverse wave) compared to the dynamics in k_{η} and η .

Consider first a quasi-longitudinal wave. In this case, one can find the longitudinal dynamics approximately by fixing values of k_R and R and solving the resulting dispersion relation $\mathcal{D}(k_{\eta}, \eta; k_R, R) = 0$. The slow transverse dynamics in (k_R, R) variables can then be calculated either by requiring that the adiabatic invariant $I_{\eta}(k_R, R) = \oint k_{\eta} d\eta$ associated with the longitudinal ray motion is conserved or by averaging Eqs. (15) over the fast longitudinal bounces. If the magnetic field profile $\mathcal{B}(z)$ is fixed, one can find all ray trajectories localized axially while passing $R = R_0$ by considering $k_{\eta}(\eta; k_R)$; namely by solving $\mathcal{D}(k_{\eta}, \eta; k_R, R_0) = 0$ for different values of k_R . If, however, $\mathcal{B}(z)$ can also be varied to search for the localized wave trajectories, the problem becomes much more complex. This problem can be simplified by noticing that in the lowest order α and β depend on \mathcal{B} but not on its higher derivatives. Assuming also that the plasma temperature and the line density of the plasma are constant along the device [42], one can see that $\mathcal{D}(k_{\eta}, \eta; k_R, R)$ depends on η through $\mathcal{B}(\eta)$ only. Therefore, all the information about the axially localized ray trajectories can be extracted from $k_{\eta}(\mathcal{B}; k_R)$ solving $\mathcal{D}(k_{\eta}, \mathcal{B}; k_R, R_0) = 0$. While details of this method and its application to the search for weakly-damped axially- and radially-localized modes can be found in Ref. 13, the essential elements of the search algorithm can be seen directly from the present reformulation.

Consider now a quasi-transverse wave. In this case, by analogy with the quasi-longitudinal wave, one can find the transverse dynamics first by fixing values of k_{η} and

η and solving the dispersion relation $\mathcal{D}(k_R, R; k_{\eta}, \eta) = 0$. The slow longitudinal dynamics in (k_{η}, η) variables can then be calculated from the conservation of the transverse adiabatic invariant $I_R(k_{\eta}, \eta) = \oint k_R dR$ or by averaging Eqs. (16) over the fast oscillations in (k_R, R) coordinates [the averaged equations are equivalent to Eqs. (8) and (9) of Ref. 13]. If the magnetic field profile $\mathcal{B}(z)$ is fixed, the axially-localized modes can be identified by studying a ‘‘phase portrait’’ in (k_{η}, η) coordinates. This portrait can be calculated by solving $I_R(k_{\eta}, \eta) = I$ for different values of I . In the case when the magnetic field profile \mathcal{B} is also allowed to vary, one can use the same approach employed above. Specifically, after substituting the lowest-order expressions for α and β in \mathcal{D} and assuming again that the plasma temperature and the line density are constant along the device axis, the dispersion relation will depend on η through $\mathcal{B}(\eta)$ only. Therefore, the search for axially localized ray trajectories can be performed by studying $k_{\eta}(\mathcal{B}; I)$ solving $I_R(k_{\eta}, \mathcal{B}) = I$ for various values of I . The search for weakly-damped modes can be simplified even further recalling that $k_{\parallel} \ll k_n$ for the waves of interest. In this case, assuming that the wave is localized near the midplane, one can expand \mathcal{D} in powers of k_{η} and η and consider the lowest-order terms only. This approximation and its application to the search of the quasi-transverse, axially-localized modes are similarly discussed in greater detail in Ref. 13.

V. MODES SUITABLE FOR ALPHA-CHANNELING

The quasi-longitudinal and the quasi-transverse waves suitable for α -channeling were identified in two practical open-ended fusion devices [13, 16, 17] using the methods outlined in Sec. IV. Both modes satisfied the fast wave dispersion relation reading

$$a = n_{\parallel}^2 + \frac{d^2}{b - n_{\parallel}^2 - n_{\perp}^2}, \quad (17)$$

where

$$a \approx 1 - \sum_{i,n} \frac{\omega_{pi}^2}{\omega} e^{-\lambda_i} \frac{n^2 I_n(\lambda_i)}{\lambda_i (\omega - n\Omega_i)}, \quad (18)$$

$$b \approx 1 - \sum_{i,n} \frac{\omega_{pi}^2}{\omega} \frac{e^{-\lambda_i}}{\omega - n\Omega_i} \left[\frac{n^2 I_n(\lambda_i)}{\lambda_i} + 2\lambda_i (I_n - I'_n) \right], \quad (19)$$

$$d \approx \sum_{i,n} \frac{\omega_{pi}^2}{\omega} \frac{n e^{-\lambda_i} (I_n - I'_n)}{\omega - n\Omega_i} + \frac{\omega_{pe}^2}{\omega \Omega_e}. \quad (20)$$

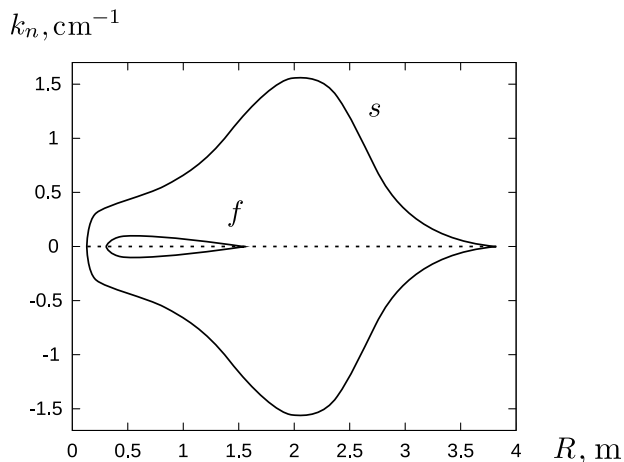


FIG. 2: The dependence of k_n on R for the quasi-longitudinal and the quasi-transverse waves. The quasi-longitudinal wave is marked with “s”, while the quasi-transverse trajectory is marked with “f”.

Here $n_{\parallel} = k_{\parallel}c/\omega$, $n_{\perp} = k_{\perp}c/\omega$, $I_n = I_n(\lambda_i)$ is the modified Bessel function of the first kind, and for each species s , ω_{ps}^2 is the plasma frequency, $w_{s\parallel}$ and $w_{s\perp}$ are parallel and perpendicular thermal particle velocities correspondingly, $\lambda_s = k_{\perp}^2 \rho_s^2 / 2$, $\rho_s = w_{s\perp} / \Omega_s$, and Ω_s is the particle gyrofrequency. The quasi-longitudinal and quasi-transverse waves had similar longitudinal wave lengths, the former, however, was characterized by larger k_{\perp} (see Fig. 2).

Ray trajectories simulated for the identified waves were shown [13] to be localized both axially and radially (see Fig. 3). The quasi-longitudinal wave propagated in a larger radial range compared to the quasi-transverse wave (see Fig. 2) reaching the device periphery, where the plasma density was 5 to 6 orders of magnitude smaller compared to the device core. Thus, it should be possible to couple the quasi-longitudinal mode to an externally placed antenna.

Now that we have identified suitable modes for accomplishing the α -channeling effect, it remains to suggest how to validate these assertions through proof-of-principle experiments on existing open-ended devices. One device suitable for such experiments might be the Large Plasma Device (LAPD) located in the University of California, Los Angeles [18]. In fact, using the collisionless kinetic dispersion relation employed to identify α -channeling modes in Ref. 13, a similar quasi-longitudinal mode can be shown to exist in the LAPD device. However, since the characteristic collisional frequencies are comparable to the ion cyclotron frequency in the LAPD

plasmas, the effect of collisions on the mode dispersion relation may need to be accounted for before a definitive experiment can be proposed. Such an experiment would provide an existence proof of a mode with suitable characteristics for accomplishing the α -channeling effect, even if the wave-particle interaction per se of cooling fast ions is not performed. Of course, as a next step, the interaction of this mode with energetic ions (simulating α particles) could be contemplated.

VI. CONCLUSION AND DISCUSSION

In summary, by arranging diffusion paths in phase space and performing a rough optimization of α -channeling efficiency with respect to the rf region parameters, we showed that among various topologies the highest α -channeling efficiency can be reached for the system of paths shown on Fig. 1. Specifically, up to 60% of the total α particle energy can, in principle, be extracted for this configuration from a practical open-ended fusion device on a time much smaller than a characteristic collisional energy relaxation time. In reaching this optimization, we did restrict ourselves to paths in which the resonance condition is maintained throughout the particle diffusion; this restricted the solution space to long parallel wavelengths. A more general consideration might allow for shorter wavelength modes, but then an intersecting network of diffusion paths would need to be used so that particles diffuse to the point of ejection. Such a consideration would be a more complicated, but certainly feasible.

With this restriction noted, we identified the region of the wave parameter space in which the α -channeling efficiency is optimized. We can then search for plasma waves satisfying these restrictions. In so doing, we identified a quasi-longitudinal wave propagating primarily along the magnetic field lines, as well as a quasi-transverse wave propagating in a perpendicular direction. Here, in discussing these results, using a more convenient set of coordinates than that used in Ref. 13, we also rederived the method of the wave search.

In addition to the restriction on wavelength, the plasma configuration considered so far is simple; more complicated configurations of plasma may permit other wave candidates. Thus, while an extensive search of suitable waves was conducted, other candidate modes, possibly superior to the ones identified here, may in fact exist, and remain to be discovered.

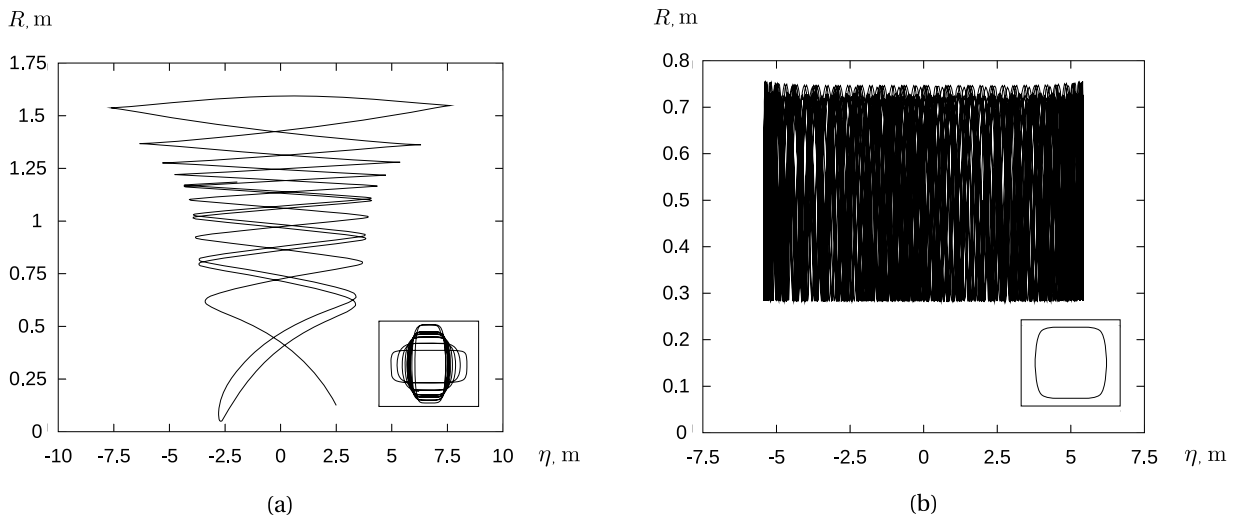


FIG. 3: A sample spatial projection of the ray trajectory for (a) the quasi-longitudinal and (b) the quasi-transverse waves. The insets show the characteristic dependencies of k_{\parallel} on η .

In any event, although the waves found here are for the simple mirror geometry, the method of finding the waves, and indeed the waves themselves, may be more generally applicable. In particular, the method of identifying the weakly-damped modes suitable for α -channeling and the modes themselves might also be useful for implementing α -channeling [26, 27] in magnetic mirror traps with supersonic rotation [28–34]. These traps of rotating plasma might be useful for fusion energy generation or for isotope separation.

It should be noted that although we found certain modes suitable for α -channeling, we have not quite demonstrated, even numerically, a complete scenario for α -channeling in practical mirror machines. It does remain to find the mode structure in the case when the geometrical optics approximation fails (since the large longitudinal wave length might be comparable to the device length). Also, the fraction of affected α particles and the expected α -channeling efficiency should be determined. This is particularly important when there is only one or two rf regions in the system and their longitudinal mode numbers are small, in which case the corresponding diffusion paths are wide and the resulting particle evolution might differ significantly from that simulated in Ref. 14.

Also, the methods used here to find waves suitable for α -channeling do not take into account non-ideal effects. The main non-ideal effects ignored here, namely those due to particle collisions, may not be important for a reactor, but may be important in demonstrating proof-of-principle experiments on LAPD or other similar low-

temperature devices.

Note that it is important to retire whatever questions we can on existing devices, even if the full rf cooling and channeling effect cannot be produced on existing devices. In this respect, the program in mirror machines might be compared to what has been accomplished in tokamaks. In tokamaks, a similar ion wave was identified as being useful, namely the mode converted ion Bernstein wave [35, 36]. This wave was then seen to have many of the key, required characteristics on an existing device, the TFTR tokamak, even though the full channeling effect could not be explored in the absence of α particles. However, when experiments on TFTR were carried out [37], the surprise was that the diffusion operated more rapidly than predicted by an astounding factor of about 50, thereby suggesting the presence of contained modes [38, 39]. The supposition was then that the contained modes were excited by coupling to the mode converted ion Bernstein wave.

Although the excitation of contained modes was a surprise in the tokamak campaign, in the case here of open geometry mirror machines, our search actually begins directly with the study of the contained modes, which produce the largest diffusion for a given injected power. Like for tokamaks, although the method of excitation is different, the most suitable modes appear to be eigenmodes in the ion cyclotron range of frequencies. In addition, like in the tokamak program, in identifying here these suitable contained modes on mirror machines, we can propose searching experimentally on presently available

devices for the presence of modes with key attributes for α -channeling, thereby motivating further exploration of the possibilities of this important effect in open geometries.

VII. ACKNOWLEDGMENTS

This work was supported by DOE Contracts No. DE-FG02-06ER54851 and DE-AC0276-CH03073.

-
- [1] G. H. MILEY, *Phys. Scripta* **T16**, 58 (1987).
- [2] J. D. HANSON and E. OTT, *Phys. Fluids* **27**, 150 (1984).
- [3] G. R. SMITH, *Phys. Fluids* **27**, 1499 (1984).
- [4] G. R. SMITH, W. M. NEVINS, and W. M. SHARP, *Phys. Fluids* **27**, 2120 (1984).
- [5] R. G. L. VANN, H. L. BERK, and A. R. SOTO-CHAVEZ, *Phys. Rev. Lett.* **99**, 025003 (2007).
- [6] H. L. BERK, *Transp. Theory Stat. Phys.* **34**, 205 (2005).
- [7] H. L. BERK, C. J. BOSWELL, D. BORBA, A. C. A. FIGUEIREDO, T. JOHNSON, M. F. F. NAVE, S. D. PINCHES, and S. E. SHARAPOV, *Nucl. Fusion* **46**, S888 (2006).
- [8] D. A. GATES, N. N. GORELNIKOV, and R. B. WHITE, *Phys. Rev. Lett.* **87**, 205003 (2001).
- [9] J. F. CLARKE, *Nucl. Fusion* **20**, 563 (1980).
- [10] W. R. SUTTON, D. J. SIGMAR, and G. H. MILEY, *Fusion Tech.* **7**, 374.
- [11] T. K. FOWLER and M. RANKIN, *J. Nucl. Energy, Part C* **8**, 121 (1966).
- [12] N. J. FISCH, *Phys. Rev. Lett.* **97**, 225001 (2006).
- [13] A. I. ZHMOGINOV and N. J. FISCH, *Phys. Plasmas* **16**, 112511 (2009).
- [14] A. I. ZHMOGINOV and N. J. FISCH, *Phys. Plasmas* **15**, 042506 (2008).
- [15] N. J. FISCH, *Fusion Sci. Technol.* **51**, 1 (2007).
- [16] J. PRATT and W. HORTON, *Phys. Plasmas* **13**, 042513 (2006).
- [17] J. PRATT, W. HORTON, and H. L. BERK, *Journal of Fusion Energy* **27**, 91 (2008).
- [18] W. GEKELMAN et al., *Rev. Sci. Instrum.* **62**, 2875 (1991).
- [19] N. J. FISCH and J. M. RAX, *Phys. Rev. Lett.* **69**, 612 (1992).
- [20] A. J. LICHTENBERG and M. A. LIEBERMAN, *Regular and Chaotic Dynamics* (second ed., Springer-Verlag, New York, 1992).
- [21] G. R. SMITH and A. N. KAUFMAN, *Phys. Fluids* **21**, 2230 (1978).
- [22] A. I. ZHMOGINOV and N. J. FISCH, *Phys. Lett. A*, **372**, 5534 (2008).
- [23] T. H. STIX, *Waves in Plasmas* (Springer-Verlag, New York, 1992), Chapter 15.
- [24] T. H. STIX, *Waves in Plasmas* (Springer-Verlag, New York, 1992), Chapter 17.
- [25] I. KATANUMA, Y. TATEMATSU, K. ISHII, T. TAMANO, and K. YATSU, *J. Phys. Soc. Jap.* **69**, 3244 (2000).
- [26] A. J. FETTERMAN and N. J. FISCH, *Phys. Rev. Lett.* **101**, 205003 (2008).
- [27] A. J. FETTERMAN and N. J. FISCH, *Plasma Sources Sci. and Tech.* **18**, 045003 (2009).
- [28] B. LEHNERT, *Nucl. Fusion* **11**, 485 (1971).
- [29] B. LEHNERT, *Phys. Scripta* **9**, 189 (1974).
- [30] A. A. BEKHTENEV, V. I. VOLOSOV, V. E. PAL'CHIKOV, M. S. PEKKER, and Y. N. YUDIN, *Nucl. Fusion* **20**, 579 (1980).
- [31] B. BONNEVIER, *Arkiv Fysik* **33**, 255 (1967).
- [32] B. BONNEVIER, *Plasma Phys.* **13**, 763 (1971).
- [33] M. KRISHNAN, M. GEVA, and J. HIRSCHFELD, *Phys. Rev. Lett.* **46**, 36 (1981).
- [34] T. OHKAWA and R. MILLER, *Phys. Plasmas* **9**, 5116 (2002).
- [35] E. J. VALEO and N. J. FISCH, *Phys. Rev. Lett.* **73**, 3536 (1994).
- [36] N. J. FISCH, *Phys. Plasmas* **6**, 2375 (1995).
- [37] N. J. FISCH, *Nuclear Fusion* **40**, 1095 (2000).
- [38] M. C. HERRMANN, *Cooling Alpha Particles with Waves*, P.D. Thesis, Princeton University (1998).
- [39] D. S. CLARK and N. J. FISCH, *Phys. Plasmas* **7**, 2923 (2000).
- [40] Recall that the basis vectors $\vec{e}_R = \partial/\partial R$ and $\vec{e}_\eta = \partial/\partial\eta$ are such vectors that the derivative of any function f along them is equal to $\partial f/\partial R$ and $\partial f/\partial\eta$ correspondingly.
- [41] Alternatively, k_R and k_η can be calculated by recalling that $k \in T_q^*M$ is a contravariant vector, where $q \in M$ is an element of the configuration space and therefore, $k_R = k_r \partial r/\partial R + k_z \partial z/\partial R$ and $k_\eta = k_r \partial r/\partial\eta + k_z \partial z/\partial\eta$.

[42] We assume that temperatures of the plasma species $T_{e/i}$ are functions of R only and that the plasma density $n_{e/i}$ is given by $n_{e/i} \approx n_{e/i}^0(R) \sqrt{\mathcal{B}(\eta)/\mathcal{B}(0)}$.

The Princeton Plasma Physics Laboratory is operated
by Princeton University under contract
with the U.S. Department of Energy.

Information Services
Princeton Plasma Physics Laboratory
P.O. Box 451
Princeton, NJ 08543

Phone: 609-243-2245
Fax: 609-243-2751
e-mail: pppl_info@pppl.gov
Internet Address: <http://www.pppl.gov>